The Late Jurassic to present evolution of the Andean margin: Drivers and the geological record

Kayla T. Maloney,[1] Geoffrey L. Clarke,[1] Keith A. Klepeis,[2] and Leonardo Quevedo[1]

[1]   Uncommonly long-lived subduction and variable plate geometry along the South American Andean Plate margin resulted in diverse relationships between magmatic flux and extensional and contractional deformation, as recorded by the overriding continental plate. Convergence velocities, absolute overriding plate velocities, and subducting slab ages were resolved along the trench from 170 Ma to the present using a recently developed kinematic global plate model to identify any relationship between subduction conditions, deformation style, and magmatic features in the overriding plate. Key correlations reflect the dependence of macroscopic crustal strain style on subduction mechanism and relative plate vectors. Extensional back-arc basins involving mafic/oceanic crust developed only when the overriding plate velocity of South America was directed away from the trench and the modeled age of the subducting slab was older than 50 Myr. The development of fold and thrust belts, and uplift of major plateaus, was accompanied by trench normal convergence velocities in excess of 4 cm/yr. Parameters investigated in this study revealed no correlation with the timing of major magmatic events, nor was any correlation observed with the structural style of fold and thrust belts.

1.   Introduction

[2]   The Andean margin of South America is commonly considered the type example of an ocean-continent convergent margin. Initially situated along the southwestern margin of Gondwana prior to its dispersal, this margin has been the site of subduction since at least the Jurassic [*James*, 1971; *Coira et al.*, 1982; *Pankhurst et al.*, 2000; *Oliveros et al.*, 2006]. During this long-lived subduction, the Andean margin developed a varied and commonly complex sequence of superimposed deformation and magmatic events. This paper examines relationships between conditions imposed on the margin by the subduction zone(s) and the development of specific significant geological events in the arc and back-arc regions of the overriding South American Plate over the past 170 Ma. Geological events identified in this analysis needed to be of sufficient magnitude to have been influenced by plate-scale processes, with reasonable control on their timing and duration.

[3]   The influence of any given subduction zone(s) on deformation in the overriding plate has been investigated along the South American margin by various authors. Numerous conditions have been implicated as drivers of deformation and magmatism, including the rate of convergence between subducting and overriding plates [*Pilger*, 1984; *Yáñez and Cembrano*, 2004; *Capitanio et al.*, 2011; *Ramos*, 2010; *Daly*, 1989; *Pindell and Tabbutt*, 1995], the absolute velocity of South America in a mantle or hot spot reference frame [*Ramos*, 2010; *Yáñez and Cembrano*, 2004; *Martinod et al.*, 2010; *Pindell and Tabbutt*, 1995], the model age of the subducting slab [*Capitanio et al.*, 2011; *Yáñez and Cembrano*, 2004; *Pilger*, 1984; *Pindell and Tabbutt*, 1995], the dip of the subducting slab [*Pilger*, 1981, 1984; *Jarrard*, 1986; *Lallemand et al.*, 2005; *Martinod et al.*, 2010], trench velocity [*Pindell and Tabbutt*, 1995; *Oncken et al.*, 2006; *Ramos*, 2010], and the lateral width of the subducting slab [*Schellart*, 2008; *Schellart et al.*, 2007]. The relative influence of each of these various conditions on deformation is unclear, as are the effects of any potential interactions between the conditions. As yet no single parameter has been satisfactorily identified as a primary controller of overriding plate deformation, implying that interaction between the conditions likely plays an important role in determining tectonic regime and deformation style.

[4]   A well-constrained data set is essential in elucidating relationships between subduction zone dynamics and the geological evolution of the overriding South American Plate. The identification of plausible correlations between subduction parameters and deformation requires that the initiation and duration of any deformation event be precisely constrained. Recent advances in dating techniques have provided refined constraints on event ages. In addition,

[1]School of Geosciences, University of Sydney, Sydney, New South Wales, Australia.
[2]Department of Geology, University of Vermont, Burlington, Vermont, USA.

Corresponding author: K. T. Maloney, School of Geosciences, University of Sydney, City Rd., Sydney, NSW 2006, Australia. (kayla.maloney@sydney.edu.au)

data from recent field studies [e.g., *Villagómez et al.*, 2011; *McAtamney et al.*, 2011] have provided an improved understanding of key parts of the Andean margin and more detail in the nature and timing of deformation and magmatic events.

[5] A recently developed global plate kinematic model [*Seton et al.*, 2012] allows the reconstruction of tectonic plate configuration back to 200 Ma. It was used to investigate relationships between subduction and geologic events recorded by the overriding South American Plate. A hybrid absolute reference frame comprising a moving Indian/Atlantic hot spots reference frame [*O'Neill et al.*, 2005] from 100 Ma to the present and a paleomagnetically derived true polar wander corrected reference frame [*Steinberger and Torsvik*, 2008] back to 200 Ma is used for the model, with the Pacific reference frame modified from *Wessel and Kroenke*'s [2008] fixed Pacific hot spots to remove certain unrealistically fast plate motions. This model incorporates the breakup of the Ontong-Java, Hikurangi, and Manihiki Plateaus [*Taylor*, 2006] in the South Pacific, which has repercussions in the calculated locations of ridge subduction and oceanic plate velocities experienced by the Andean margin. The model and associated oceanic crust age grid [*Seton et al.*, 2012] were used to investigate convergence rates, the absolute motion of South America, and the ages of subducting slabs in relation to the timing of the development of extensional basins, fold and thrust belts, uplift of the Altiplano-Puna Plateau, and major magmatic events. This method implicitly accepts the kinematic model; uncertainties with respect to plate position and motion increase with age, particularly in the Pacific region. The model was not itself explicitly tested. However, a first-order evaluation of the modeling outcomes is provided by the geological record, as discussed below. Though slab dip and mantle flow are commonly considered significant parameters influencing geometry, plate coupling, and tectonic setting [*Jarrard*, 1986; *Ramos*, 2010], they were omitted from this study as there are no accurate models of dip or mantle flow patterns back through time developed independently of the geology of the margin.

2. Overview of Deformation in the Andes

[6] The effects of post-Jurassic deformation along the western margin of South America can be placed into either of two broad categories: extension during the Late Jurassic and Cretaceous, and contraction from the Late Cretaceous to the present (Figure 1). The margin is divided into five regions: northern, Peruvian, central, south-central, and southern Andes. This arbitrary division simply facilitates the discussion and evaluation of complex detail in the history of the Andean margin and highlights any dependence between particular geological events and the edge of a subduction zone in the geological evolution of the region.

2.1. Northern Andes (8°N to 5.5°S)

[7] The region defined here as the northern Andes extends from Colombia to northern Peru. Tectonic style in the region was influenced by its interaction with the Caribbean Plate system [*Pindell and Kennan*, 2009]. The northern Andean margin comprises a series of accreted and para-autochthonous terranes assembled during the late Mesozoic juxtaposed against autochthonous continental crust [*McCourt et al.*, 1984;

Nivia et al., 2006; *Villagómez et al.*, 2011]. Extension and lithospheric thinning of the margin occurred from the Late Jurassic to Early Cretaceous. The igneous Quebradagrande Complex consists of both mid-ocean ridge basalt and arc-related rocks, erupted through attenuated crust [*Villagómez et al.*, 2011]. This event resulted in the Colombian Marginal Seaway (8°N–5.5°S), a circa 140–130 Ma north trending basin floored by oceanic crust. The basin has been extrapolated to the proposed Proto-Caribbean Seaway, which began to close by circa 100 Ma [*Kennan and Pindell*, 2009; *Aspden and McCourt*, 1986; *Nivia et al.*, 2006]. Shortening in the early Cenozoic led to out-of-sequence reactivation of Mesozoic extensional rifts in and uplift the Eastern Cordillera of Colombia (6°N–2°N) at circa 60–20 Ma [*Parra et al.*, 2009a, 2009b, 2012].

2.2. Peruvian Andes (5.5°S to 14°S)

[8] The region defined here as the Peruvian Andes extends from northern to southern Peru, terminating at the start of the Altiplano-Puna Plateau. Late Jurassic and Cretaceous extension continued along this portion of the margin and led to the Tithonian (circa 147 Ma) [*Gradstein et al.*, 1994] aged opening of the Huarmey and Cañete Basins [*Cobbing*, 1978; *Atherton and Aguirre*, 1992]. Sheeted mafic dyke swarms and pillow lavas in the Huarmey Basin (8°S–12°S) are interpreted to reflect extensive crustal extension [*Atherton et al.*, 1983], on a scale inadequate to form new oceanic crust [*Ramos*, 2010]. Crustal extension without the development of new oceanic crust also formed the Cañete Basin (12°S–16°S) [*Atherton and Aguirre*, 1992]. The main phase of subsidence in both basins occurred in the Albian (circa 99 Ma) and sediment accumulation ceased soon after [*Cobbing*, 1978]. Components of the circa 105–37 Ma Peruvian Coastal Batholith include several superunits [*Mukasa*, 1986] distinct in timing and geochemistry. The most voluminous flux is recorded by parts of the circa 86–70 Ma Santa Rosa and Tiabaya superunits [*Mukasa*, 1986]. Cenozoic contraction first developed in this region with the middle to late Eocene thin-skinned Marañon fold and thrust belt (7°S–12.5°S). Reactivation of these thrusts occurred during a second phase of contraction from circa 20 to 13 Ma [*Mégard*, 1984]. The locus of deformation then shifted eastward at circa 11 Ma to the presently active thin-skinned northern Peruvian Sub-Andean fold and thrust belt (3°S–11°S) [*Audebaud et al.*, 1973; *Rousse et al.*, 2003; *Mégard*, 1984]. To the west of these fold and thrust belts, the circa 13–3 Ma Cordillera Blanca Batholith was emplaced approximately 100 km inboard of the Peruvian Coastal Batholith [*Atherton and Petford*, 1996]. Detachment faulting along the western flank of the Cordillera Blanca Batholith beginning at circa 5 Ma resulted in the still active extensional Callejon de Huaylas Basin (8.5°S–10°S) [*Giovanni et al.*, 2010; *McNulty and Farber*, 2002]. The Callejon de Huaylas Basin is one of only a handful of locations along the margin to record Cenozoic extension (Figure 1).

2.3. Central Andes (14°S to 34°S)

[9] The region defined here as the central Andes comprises the Altiplano-Puna Plateau and the adjacent foreland of southernmost Peru, extending through northern and central Chile to western parts of Argentina. The southern portion of the Cañete Basin and the southernmost units of the Peruvian Coastal Batholith both extend southward into this
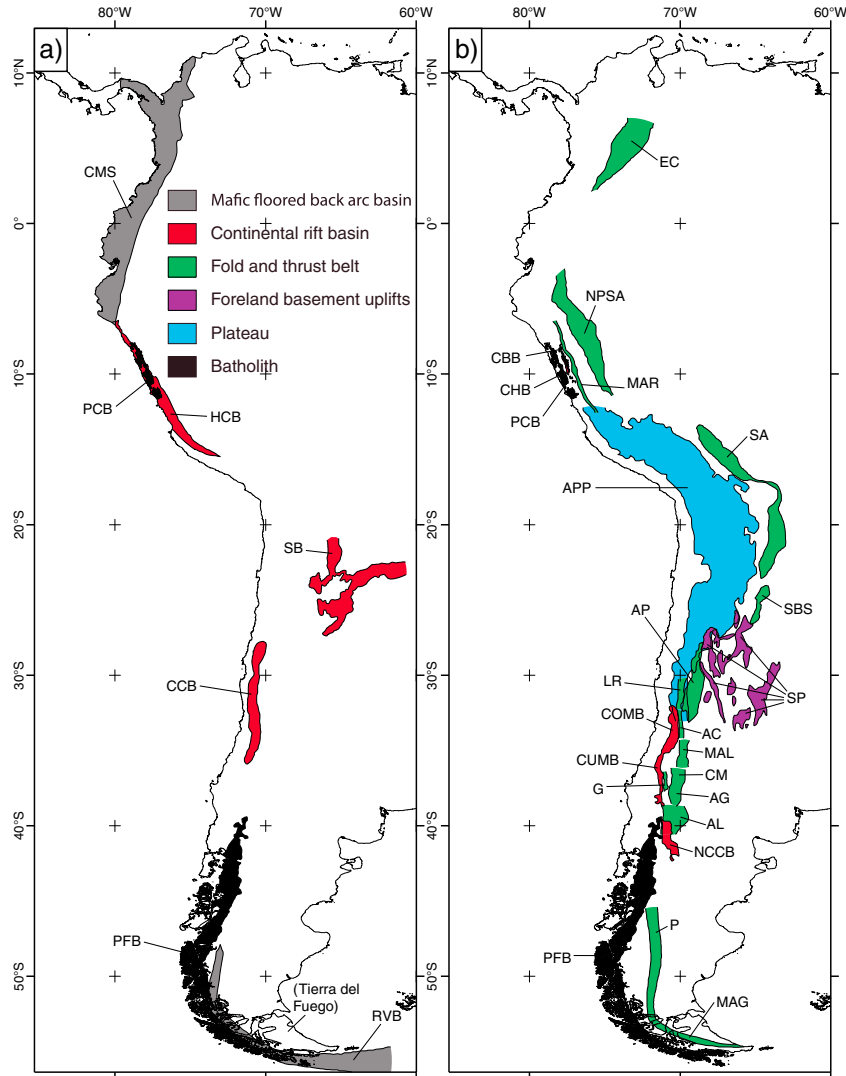
Figure 1. (a) Late Jurassic to Cretaceous deformation and magmatic events along the Andean margin. Note that as much of the crust flooring the mafic back-arc basins is no longer extant the outlines shown are interpreted potential extents. In the case of the Rocas Verdes Basin, the northernmost ophiolite fragments are reported at 52°S, so this has been used as the northernmost point in the analysis, but the basin may have stretched farther north. CMS: Colombian Marginal Seaway, PCB: Peruvian Coastal Batholith, HCB: Huarmey and Cañete Basins, SB: Salta Basin, CCB: Central Chilean Basin, PFB: Patagonian and Fuegian Batholiths, RVB: Rocas Verdes Basin. (b) Cenozoic deformation and magmatic events along the Andean margin. EC: Eastern Cordillera of Colombia, NPSA: North Peruvian Sub-Andean fold and thrust belt (FTB), MAR: Marañon FTB, CBB: Cordillera Blanca Batholith, CHB: Callejon de Huaylas Basin, PCB: Peruvian Coastal Batholith, APP: Altiplano-Puna Plateau, SA: Sub-Andean FTB, SBS: Santa Bárbara System, AP: Argentine Precordillera, SP: Sierras Pampeanas, AC: Aconcagua FTB, LR: La Ramada FTB, MAL: Malargüe FTB, CM: Chos Malal FTB, G: Guañacos FTB, AG: Agrio FTB, COMB: Coya-Machalí Basin, CUMB: Cura Mallín Basin, AL: Aluminé FTB, NCCB: Ñirihuau-Collón Curá Basin, PFB: Patagonian and Fuegian Batholiths, P: Patagonian FTB, MAG: Magallanes FTB. Data sources include *Ramos et al.* [1996], *Hervé et al.* [2007], *Atherton and Petford* [1996], *Kley and Monaldi* [2002], *Fosdick et al.* [2011], *Ramos et al.* [2002], *Klepeis and Austin* [1997], *Gubbels et al.* [1993], *Allmendinger et al.* [1997], *Atherton and Aguirre* [1992], *Marquillas et al.* [2005], *Zapata and Folguera* [2005], *Vietor and Echtler* [2006], *Mégard* [1984], *Spalletti and Dalla Salda* [1996], *García Morabito and Ramos* [2012], *Paredes et al.* [2009], *Ramos and Kay* [2006], *Mora et al.* [2009], and *Giovanni et al.* [2010].

part of the Andes. Cretaceous extension resulted in the opening of the circa 130–70 Ma continental Salta Basin (22°S–27.5°S) comprising a series of seven subbasins radiating from a central high [*Marquillas et al.*, 2005; *Carrera et al.*, 2006; *Reyes*, 1972] and, immediately to the south, the opening of the Central Chilean Basin (27°S–34°S) during Aptian and Cenomanian (circa 120–94 Ma) times [*Mpodozis and Allmendinger*, 1993; *Levi and Aguirre*, 1981].

[10] The Altiplano-Puna Plateau of the central Andes is second only to the Tibetan Plateau in height and extent, and is the highest plateau associated with abundant and ongoing arc magmatism [*Allmendinger et al.*, 1997]. It is divided into two regions based on distinctions in uplift history and morphology: the Altiplano portion to the north (14°S–22°S) and the higher Puna portion to the south (22°S–28°S) [*Whitman et al.*, 1996; *Isacks*, 1988]. South of the Puna Plateau, Andean altitudes remain higher than 3 km to circa 34°S [*Whitman et al.*, 1996; *Allmendinger et al.*, 1997]. Crustal uplift to form the Altiplano may have begun as early as the Eocene, but most uplift is thought to have occurred between circa 25 and 12 Ma. Uplift of the Puna Plateau commenced between circa 20 and 15 Ma and continued until circa 2–1 Ma [*Allmendinger et al.*, 1997]. This region has the thickest crust of the Andean margin, being circa 60–65 km thick beneath the Altiplano and approximately 10 km thinner beneath the Puna portion [*Beck et al.*, 1996; *Beck and Zandt*, 2002; *Gerbault et al.*, 2005].

[11] On the eastern flank of the Altiplano, in the Eastern Cordillera, the thick-skinned reactivation of earlier Paleozoic compressive and Mesozoic extensional structures is interpreted to have occurred between circa 40 and 20 Ma; the locus of deformation is inferred to have migrated eastward after 20 Ma to develop a thin-skinned Sub-Andean fold and thrust belt that is still active [*McQuarrie et al.*, 2005; *Gubbels et al.*, 1993; *Burchfiel et al.*, 1981; *Isacks*, 1988]. The continuous nature of the Sub-Andean fold and thrust belt, which developed along the length of the Altiplano, contrasts with the varied deformation fabrics in foreland crustal material adjacent the Puna portion of the plateau. The Puna foreland comprises several fold and thrust belts and basement terranes of distinct style and age. Flat slab subduction of the Nazca Plate between 27°S and 33°30′S [*Barazangi and Isacks*, 1976] introduced further tectonic complexity in deformed rocks of the southernmost Puna foreland. A structural inversion of the Cretaceous Salta Basin began after circa 9 Ma [*Reynolds et al.*, 2000] to form the thick-skinned thrust belt of the Santa Bárbara System (23°S–27°S) at the northern limit of flat slab subduction [*Grier et al.*, 1991; *Kley and Monaldi*, 2002]. The influence of flat-slab subduction of the Nazca Plate is also seen in foreland basement uplifts of the Sierras Pampeanas (27°S–33.5°S) where large basement blocks were uplifted in the late Cenozoic, starting from circa 7 Ma [*Ramos et al.*, 2002]. Directly west of the Sierras Pampeanas, thin-skinned thrusting in the Argentine Precordillera (28°S–33°S) developed along a Cambo-Ordivician limestone detachment surface starting at circa 21 Ma [*Jordan et al.*, 1993; *Vietor and Echtler*, 2006]. To the west and south of the Argentine Precordillera, a string of fold and thrust belts developed in close proximity, and at about the same time, but display distinct structural styles. The La Ramada fold and thrust belt (31.5°S–32.5°S) records alternating episodes of thin- and thick-skinned thrusting [*Cristallini and Ramos*, 2000].

Thin-skinned thrusting, involving a detachment floored by evaporites, occurred between circa 20 and 14 Ma. The reactivation of Triassic normal faults then led to thick-skinned style deformation between circa 14 and 12.7 Ma. This produced a sticking point in the foreland propagation of orogeny and resulted in out-of-sequence thin-skinned thrusting on the west side of the belt between circa 12 and 9.2 Ma [*Cristallini and Ramos*, 2000; *Ramos et al.*, 1996]. Thin-skinned thrusting in the Aconcagua fold and thrust belt (32.5°S–34°S) began at circa 22 Ma, coeval with, or just prior to, uplift in the Puna Plateau, and continued until circa 8 Ma [*Ramos et al.*, 1996; *Ramos*, 1985].

2.4. South-Central Andes (34°S to 42.5°S)

[12] The region defined here as the south-central Andes extends south from the termination of the Puna Plateau through to central Chile. Widespread extension and rifting took place in this region prior to the period investigated in the study with the opening of the Triassic Neuquén Basin [*Vergani et al.*, 1995], and reactivation of these structures plays an important role in the later tectonic evolution of the region. An early phase of contractional deformation in the late Mesozoic resulted in the formation of a series of fold and thrust belts. The northernmost of these, the Chos Malal fold and thrust belt (36°S–37.5°S), records thin-skinned deformation with a detachment surface along Late Jurassic evaporites [*Folguera et al.*, 2007]. Timing of deformation in the belt is poorly constrained to sometime between the middle to Late Cretaceous, with a pulse of uplift recorded at circa 70 Ma [*Burns*, 2002; *Burns et al.*, 2006; *Kay et al.*, 2006]. Following south from the Chos Malal belt, the Agrio fold and thrust belt (37.5°S–38.5°S) records a combination of deformation styles from circa 102 to 70 Ma with thick-skinned reactivation of Neuquén Basin normal faults in the inner sector and thin-skinned thrusting in the outer, forelandward sector [*Zamora Valcarce et al.*, 2006; *Zapata and Folguera*, 2005]. Reactivation of Neuquén Basin faults is also recorded from at least circa 75 to 65 Ma in the thick-skinned Aluminé fold and thrust belt (38.5°S–40.5°S) [*García Morabito and Ramos*, 2012].

[13] This region records Cenozoic (Oligocene-Miocene) extension in a string of basins, with rare equivalent structures elsewhere along the margin. Active extensional faulting in the northernmost basin, the Coya-Machalí Basin (33°S–36°S), took place from circa 34 to 23 Ma [*Charrier et al.*, 2002; *Godoy et al.*, 1999]. Farther south, extension in the Cura Mallín Basin (36°S–38°S) occurred from circa 26 to 20 Ma [*Burns et al.*, 2006; *Jordan et al.*, 2001]. The southernmost of these basins is the circa 34–18 Ma Ñirihuau-Collón Curá Basin (40°S–42.5°S) [*García Morabito and Ramos*, 2012; *Franzese et al.*, 2011; *Rapela et al.*, 1983; *Giacosa et al.*, 2005].

[14] The Oligocene-Miocene extensional phase was followed by a period of renewed contraction that involved the development of new fold and thrust belts and the reactivation of preexisting ones. The Malargüe fold and thrust belt (34°S–36°S) developed immediately south of the Aconcagua belt (central Andes) and is characterized primarily by thick-skinned deformation [*Kozlowski et al.*, 1993; *Ramos et al.*, 1996] that involved the reactivation of extensional structures of the Triassic Neuquén Basin [*Giambiagi et al.*, 2008]. The main phase of deformation in the Malargüe fold and thrust belt occurred between circa 15 and 8 Ma,

although deformation continued until circa 1 Ma [*Giambiagi et al.*, 2008; *Turienzo*, 2010; *Ramos et al.*, 1996]. Dominantly thick-skinned reactivation in the Chos Malal fold and thrust belt occurred from circa 15 to 12 Ma and involved the inversion of Early Jurassic extensional structures as well as the reactivation of Late Cretaceous thrust faults [*Kay et al.*, 2006 *Folguera et al.*, 2007]. West of the Chos Malal belt, closure of the Cura Mallín Basin accompanied the development of the Guañacos fold and thrust belt (36.5°S–37.5°S) starting at circa 9 Ma [*Folguera et al.*, 2006; *Burns et al.*, 2006]. Deformation in this belt is predominantly thin-skinned north of 37°S, with a mix of thick- and thin-skinned styles south of 37°S [*Folguera et al.*, 2006, 2007]. South of the Chos Malal belt, the Agrio fold and thrust belt experienced thick-skinned reactivation from circa 7 to 5 Ma associated with the closure of the southern portion of the Cura Mallín Basin [*Zapata and Folguera*, 2005]. Reactivation of the Aluminé fold and thrust belt from circa 11 to 3 Ma accompanied the closure of the Ñirihuau-Collón Curá Basin [*García Morabito et al.*, 2011; *Rosenau et al.*, 2006], the southernmost of the Oligocene-Miocene extensional basins.

2.5. Southern Andes (42.5°S to 56.5°S)

[15] The region defined here as the southern Andes consists of central to southernmost Chile and central to southernmost western Argentina. It is south of the former Ñirihuau-Collón Curá Basin and extends to the southernmost point of South America. Widespread grabens and half grabens that include silicic volcanic rocks of the Tobifera Formation developed along this portion of the Andean margin between circa 178 and 153 Ma; they have been interpreted as marking the onset of Gondwana dispersal [*Bruhn et al.*, 1978; *Pankhurst et al.*, 2000].

[16] Arc-derived plutonic rocks extend continuously along the plate margin in this region to Tierra del Fuego [*Stern and Stroup*, 1982; *Hervé et al.*, 1984]. They form a distinct belt that includes the North Patagonian Batholith (40°S–47°S), the South Patagonian Batholith (47°S–53°S), and the Fuegian Batholith (53°S–56°S). Each of the batholiths formed mostly during two episodes of magma flux, of distinct ages. A first episode of the North Patagonian Batholith lasted from circa 140 to 95 Ma and a second from circa 20 to 8 Ma [*Pankhurst et al.*, 1999]. The South Patagonian Batholith mostly formed between circa 157 and 137 Ma [*Hervé et al.*, 2007], with a subsidiary episode between circa 25 and 15 Ma [*Hervé et al.*, 2007]. The circa 157 Ma episode was partially contemporaneous with silicic volcanism of the Tobifera Formation [*Hervé et al.*, 2007]. Episodic development of this batholith continued throughout much of the Cretaceous, the magma flux migrating westward with time until circa 75 Ma. The Fuegian Batholith in Tierra del Fuego records a circa 141–81 Ma episode, followed by a 20 Myr hiatus before magmatism resumed in a second episode that extended from circa 60 to 34 Ma [*Hervé et al.*, 1984; *Halpern*, 1973].

[17] The opening of the Rocas Verdes back-arc basin (52°S–56°S) at circa 152 Ma [*Calderón et al.*, 2007] was accompanied by the development of oceanic crust [*Dalziel et al.*, 1974]. Basin inversion has been inferred to be related to a change in the absolute plate motion of South America at circa 100 Ma [*Somoza and Zaffarana*, 2008; *Ramos*, 2010, this study]. By circa 92 Ma convergence had resulted in the formation of the thin-skinned Magallanes fold and thrust belt (52°S–56°S) and associated foreland basin [*Fildani et al.*, 2003; *Fildani and Hessler*, 2005; *Nelson et al.*, 1980]. The Magallanes fold and thrust belt is the southernmost segment of the Patagonian fold and thrust belt (47°S–56°S). Constraints on the timing of deformation in northern segments are poor; deformation is variously recorded to have occurred sometime between the Maastrichtian and middle Miocene (circa 71–13 Ma) in some locations [*Suárez et al.*, 2000; *Kraemer*, 1998]. Thrusting continued in the Magallanes fold and thrust belt until the late Oligocene/early Neogene [*Klepeis*, 1994]. Sinistral strike-slip faults observed in the foreland [*Cunningham*, 1993] are inferred to have dominated deformation in the region after the main thrusting events [*Klepeis*, 1994].

3. Subduction Parameters

[18] Parameters characterizing plate motion at the subduction margin were resolved at 55 points along a defined Andean trench from 170 Ma to the present. Point spacing was chosen to give good coverage of the margin. The plate model used in this study is composed of rigid, undeformable plates, with South America treated as a single rigid block such that the overriding plate velocity used in the analysis is that of the South American craton. Any smaller block rotations, such as that between Patagonia and the rest of South America, and the introduction of the Scotia Plate in southernmost South America at 40 Ma have not been considered. This oversimplification is likely valid for only some portions of the Andean margin. In regions of the Andean margin that experienced oroclinal bending, such as the Bolivian or Patagonian Oroclines, the effect of block rotations are likely to be appreciable. For instance, parts of the Patagonian Orocline record rotations of circa 90° relative to the South American craton [*Cunningham et al.*, 1991]. In these regions care must be taken when interpreting the results and the study can be viewed as an investigation of only first-order effects.

[19] The shape and position of the defined subduction trench relative to the South American craton were also kept constant. Therefore, changes in shape or position of the trench resulted in some of the 55 points being slightly offset from the actual trench position. In extreme cases, several of the northernmost points were no longer within reasonable distance of the active subduction trench; for example, some were located in the central regions of the Caribbean Plate. Therefore, data for these points after 70 Ma were ignored. As the development of the Eastern Cordillera of Colombia occurred during this interval, that event has been neglected from the analysis. Several other geologic events have necessarily been excluded from analysis due to inadequate constraints on timing of initiation and duration of the event. These excluded events include the Cretaceous-aged first episode of thrusting in the Chos Malal fold and thrust belt of the south-central Andes and the development of portions of the Patagonian fold and thrust belt of the southern Andes north of 52°S.

[20] Though South America was the only continental plate of interest, the Pacific margin interacted with several different oceanic plates. These include the Farallon, Phoenix, Chasca, Catequil, Antarctic, Nazca, and Cocos Plates; the evolving plate configuration is illustrated in Figure 2. The Chasca and Catequil Plates are new plates that are introduced in the kinematic model developed by *Seton et al.* [2012].
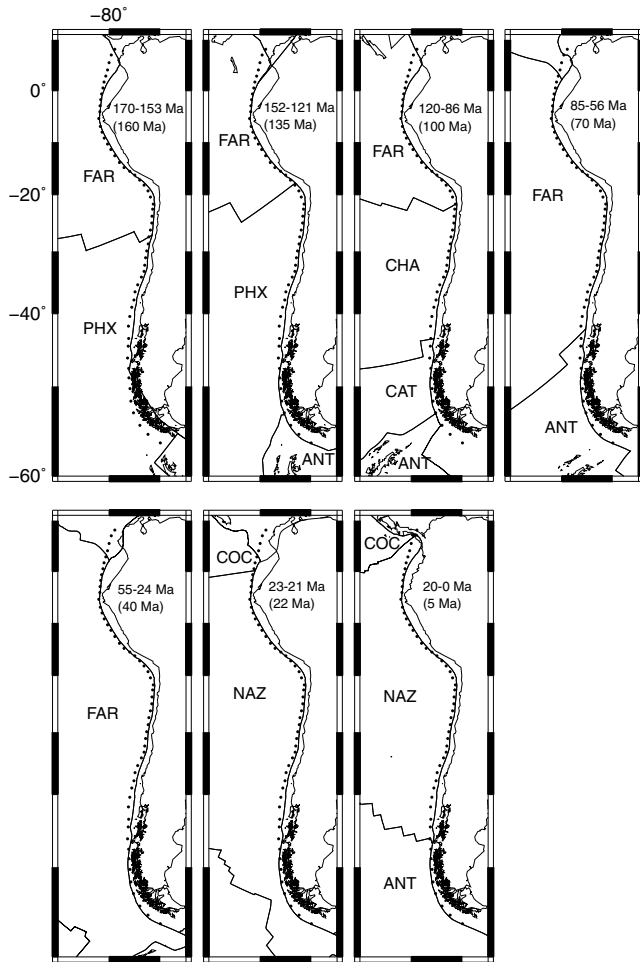
Figure 2. The various plate configurations along the Andean margin from 170 Ma to the present in a fixed South America reference frame. Time ranges for when the given configuration existed are given, while the age in brackets is the actual reconstruction age. FAR: Farallon Plate, PHX: Phoenix Plate, ANT: Antarctic Plate, CHA: Chasca Plate, CAT: Catequil Plate, COC: Cocos Plate, NAZ: Nazca Plate.

[21] Uncertainties exist in the plate configuration at the northern and southern limits of the margin, particularly at early times of the analysis. In the northern Andes, continental microplates are suggested to have existed between the present-day Colombian margin and the subduction trench [*Ross and Scotese*, 1988; *Kennan and Pindell*, 2009; *Jaillard et al.*, 1995; *Pindell and Dewey*, 1982], potentially introducing a further level of complexity in interactions between the subduction zone and South America. However, as the geometry, locations, and motions of these postulated microplates are poorly constrained [*Jaillard et al.*, 1995], and are not included in the global kinematic model, they were omitted from this analysis and only first-order effects from the subducting Farallon Plate on the overriding South American Plate were considered. At the southern end of the margin, there is a possibility that the Antarctic Peninsula may have lain immediately west of the southernmost extent of the South American Pacific margin during parts of the Mesozoic [*Lawver et al.*, 1998; *Ghidella et al.*, 2002; *Jokat et al.*, 2003; *Hervé et al.*, 2006]. Therefore, subduction might

not have occurred along the posited margin for some of the earliest times investigated, as the earliest evidence of subduction along this portion of the margin corresponds to circa 157 Ma components of the South Patagonian Batholith [*Hervé et al.*, 2007]. However, as both the position of the peninsula and the timing of exactly when overlap between the peninsula and southernmost South America ceased are poorly constrained, subduction parameters were extracted as if subduction did occur along this portion of the South American margin for the entire period investigated.

[22] The first subduction parameter is the age of the subducting slab, established by sampling the reconstructed age grid at 55 points along the defined trench; the position of a representative 10 of the 55 points is shown in Figure 3. The absolute plate velocity of South America was determined normal and parallel to the trench (Figure 4). In the case of the trench normal absolute velocity, positive values indicate that the overriding South American Plate was moving toward the trench at that time, whereas negative values reflect motion away from the trench. Trench parallel northward motion of the overriding South American Plate is indicated by positive values, and negative values indicate trench parallel motion to the south. Similarly, relative convergence velocities between South America and the various subducting oceanic slabs were determined both normal and parallel to the trench (Figure 5). Positive trench normal convergence velocities indicate convergence between South America and the subducting plate, whereas negative values indicate divergence. In the case of trench parallel convergence rates, positive values indicate right-lateral motion along the margin and negative velocities indicate that motion was left-lateral.

4. Results

[23] A comparison of model data pertinent to convergence rate, absolute plate motion, and the model ages of subducting slabs along the South America Pacific margin establishes some distinctive correlations with its geologic record, including the development of extensional basins, fold and thrust belts, uplift of plateaus, and major magmatic events (Table 1). All correlation coefficients found during the analysis are low (less than 0.39), but all have p values of much less than 1%, indicating that they are statistically significant. Low coefficients are expected. There will be errors in the attributed age and duration of recorded geological events, as well as in the oceanic crust ages and plate motions of the model used. Slab age and plate motion data become more uncertain with age. All of these factors can be expected to contribute to decreasing any correlation between the variables considered. In this context, correlations are considered strong if they have correlation coefficients with an absolute value over 0.30 (for the parameters stipulated), are considered weak for coefficients between 0.30 and 0.10, and are uncorrelated for parameters with coefficients less than 0.10.

[24] Periods of recorded crustal extension accompanied a range of tectonic scenarios. However, there is a strong correlation (coefficient 0.32) between the development of marginal basins floored by oceanic crust and the absolute motion of South America having been directed away from the trench, accompanied by the subduction of oceanic crust older than 50 Myr (Table 1), where Myr denotes million years since the crust formed at a ridge. Neither the motion
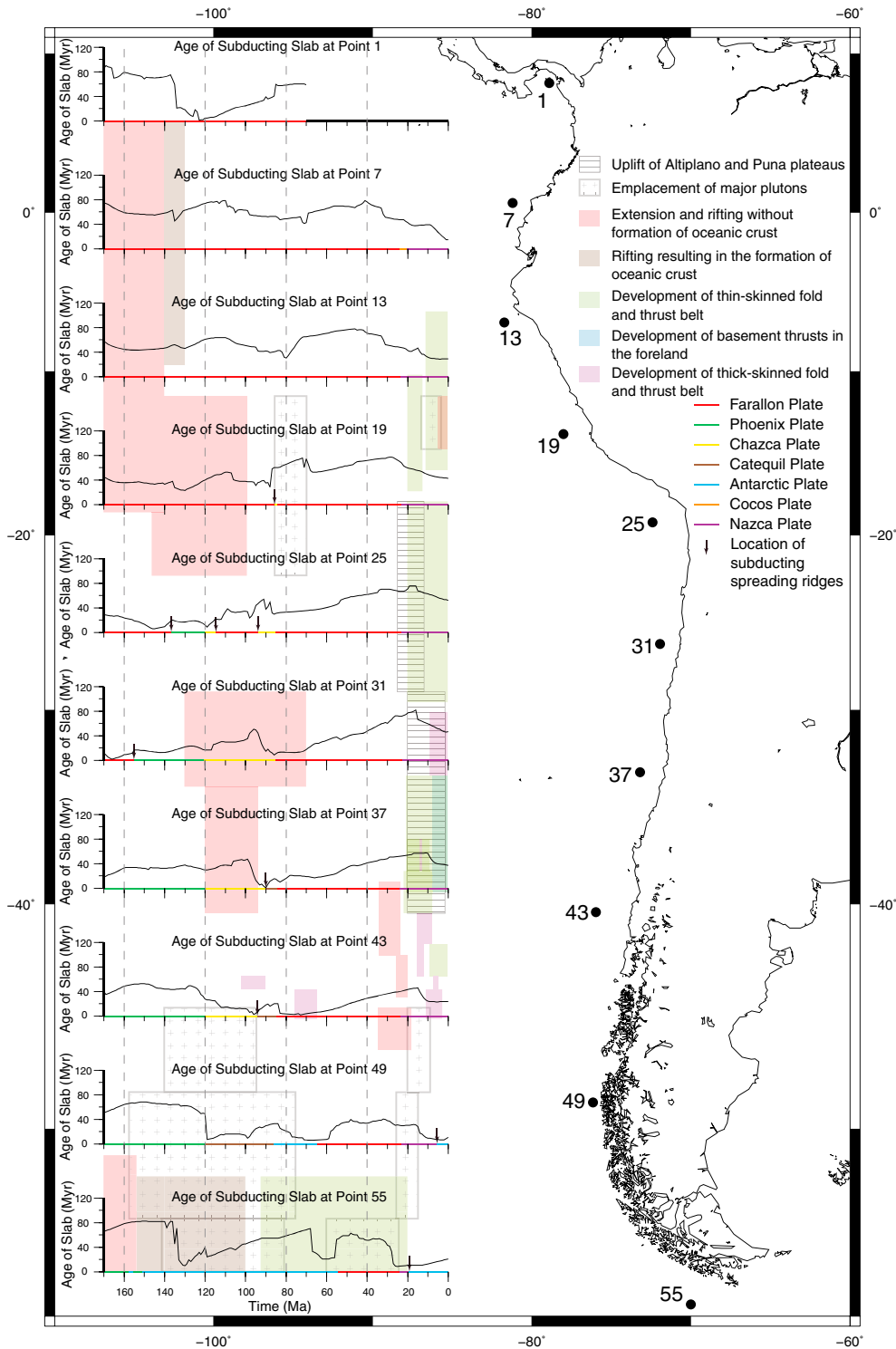
Figure 3. Age of subducting slab as a function of time for 10 of the 55 points with the duration of the deformation and magmatic events overlain on the plots. Map indicates the present-day location of the 10 points. The color of the *x* axis line indicates which slab was subducting at that location for a given time.

of South America nor the model age of the subducted slabs individually correlates well with the progression from crustal extension to back-arc spreading (Figures 3 and 4). Though east directed motion of the South American Plate occurred along much of the margin between circa 160 and 120 Ma, oceanic crust developed only at those segments of the margin where comparatively old ocean crust was subducted. Examples include the formation of the Colombian Marginal Seaway in the northern Andes and the Rocas Verdes Basin of the southern Andes (Figure 1). A strong correlation (coefficient 0.33) can also be established between these events and normal convergence velocities less than 0 cm/yr, though this
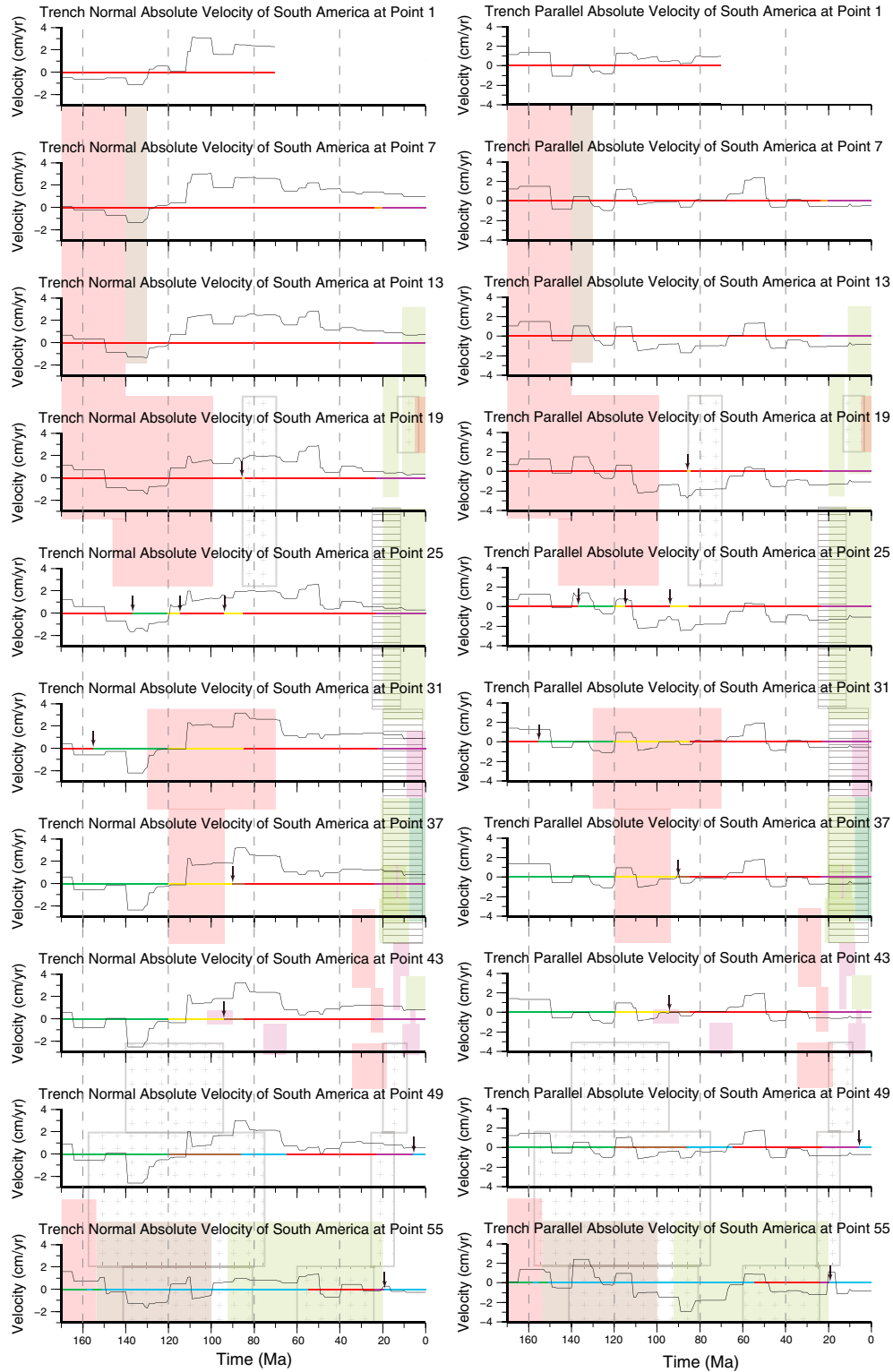
Figure 4. Trench normal absolute plate velocity of South America and trench parallel absolute plate velocity of South America as functions of time with the duration of the deformation and magmatic events overlain on the plots. Points and colors are the same as in Figure 3.

association is weakened by being absent from northern parts (north of 54.5°S) of the Rocas Verdes Basin.

[25] The development of the Altiplano-Puna Plateau of the central Andes and its flanking fold and thrust belts was accompanied by high relative trench normal convergence rates (magnitude >4 cm/yr). This relation can be extrapolated for almost all compressional events recorded by the margin. An exception is the Magallanes fold and thrust belt in the Southern Andes (Figure 1); its development was accompanied comparatively low positive or negative convergence
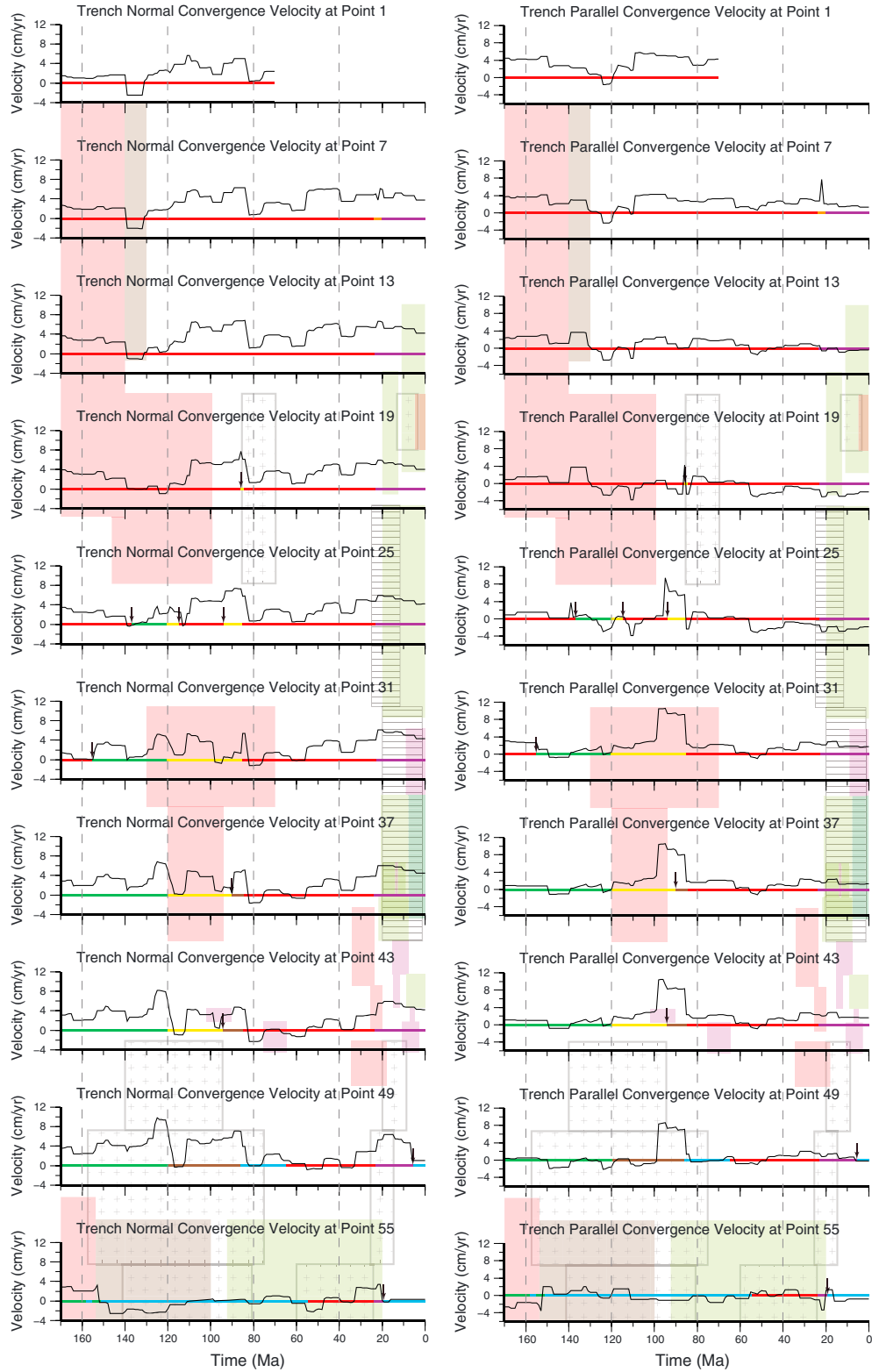
Figure 5. Trench normal convergence velocity between South America and the relevant downgoing slab, and trench parallel convergence velocity between South America and the relevant downgoing slab as functions of time with the duration of the deformation and magmatic events overlain on the plots. Points and colors are the same as in Figure 3.

Table 1. Timing, Location, and Conditions Imposed by the Subduction Zone Under Which Various Geological Events Along the Margin Developed[a,b]

Event	Location	Approximate Timing (Ma)	Normal Abs Velocity <0 cm/yr	Normal Abs Velocity >0 cm/yr	Normal Abs Velocity >2 cm/yr	Slab Age >50 Ma	Conv Velocity (Norm) <0 cm/yr	Conv Velocity (Norm) >0 cm/yr	Conv Velocity (Norm) >4 cm/yr
Continental Extension									
Sub-Andean rifting (north)	8°N to 7°S	190–140	X			X		X	
Sub-Andean rifting (south)	7°S to 14°S	190–140		X		X		X	
Huarmey and Cañete Basins	8°S to 16°S	147–99	X	X			X	X	X
Callejón de Huaylas Basin	8.5°S to 10°S	<5		X				X	X
Salta Basin	22°S to 27.5°S	130–70	X	X	X			X	
Central Chilean Basin	27°S to 34°S	120–94	X	X	X			X	
Coya-Machalí Basin	33°S to 36°S	34–23		X		X		X	
Cura Mallín Basin	36°S to 38°S	26–20		X				X	X
Ñirihuau-Collón Curá Basin	40°S to 42.5°S	34–18		X				X	
Gondwana Dispersal Rifting	50°S to 56°S	178–153	X	X		X		X	
Extension With New Oceanic Crust									
Colombian Marginal Seaway	8°N to 5.5°S	140–130	X			X	X		
Rocas Verdes Basin (north)	52°S to 54.5°S	152–100	X			X			
Rocas Verdes Basin (south)	54.5°S to 56°S	152–100	X			X	X		
Fold and Thrust Belts (FTB)									
North Peruvian Sub-Andean FTB	3°S to 11°S	<11		X				X	X
Marañon FTB	7°S to 12.5°S	20–13		X		X		X	X
Sub-Andean FTB	14°S to 22°S	<20		X		X		X	X
Santa Bárbara System	23°S to 27°S	<9		X		X		X	X
Sierras Pampeanas	27°S to 33.5°S	<8		X				X	X
Uplift									
Argentine Precordillera	28°S to 33°S	<21		X		X		X	X
La Ramada FTB	31.5°S to 32.5°S	20–9		X		X		X	X
Aconcagua FTB	32.5°S to 34°S	22–8		X		X		X	X
Malargüe FTB	34°S to 36°S	15–8(–1)[c]		X		X		X	X
Guañacos FTB	36.5°S to 37.5°S	<9		X				X	X
Chos Malal FTB	36°S to 37.5°S	15–12		X		X		X	X
Agrio FTB (1)	37.5°S to 38.5°S	102–70		X				X	X
Agrio FTB (2)	37.5°S to 38.5°S	7–5		X				X	X
Aluminé FTB (1)	38.5°S to 40.5°S	75–65		X	X			X	X
Aluminé FTB (2)	38.5°S to 40.5°S	11–3		X				X	X
Magallanes FTB	52°S to 56°S	92–20	X	X		X		X	

Table 1. (continued)

Event	Location	Approximate Timing (Ma)	Normal Abs Velocity <0 cm/yr	Normal Abs Velocity >0 cm/yr	Normal Abs Velocity >2 cm/yr	Slab Age >50 Ma	Conv Velocity (Norm) <0 cm/yr	Conv Velocity (Norm) >0 cm/yr	Conv Velocity (Norm) >4 cm/yr
Plateau Uplift									
Altiplano Plateau Uplift	14°S to 22°S	25–12		X		X		X	X
Puna Plateau and Southern Uplifts	22°S to 34°S	20–1		X		X		X	X
Magmatic Events									
Peruvian Coastal Batholith	8°S to 16°S	(105–)86–70(–37)c	X		X		X		
North Patagonian Batholith (1)	40°S to 47°S	140–95	X		X			X	X
North Patagonian Batholith (2)	40°S to 47°S	20–8		X				X	X
South Patagonian Batholith (1)	47°S to 53°S	157–75	X			X		X	X
Fuegian Batholith (1)	53°S to 56°S	141–81	X	X		X	X	X	
Fuegian Batholith (2)	53°S to 56°S	60–34		X		X	X	X	
South Patagonian Batholith (2)	47°S to 53°S	25–15						X	X
Cordillera Blanca Batholith	8°S to 10°S	13–3	X			X		X	X

[a]See text for references.

[b]Timescale from *Gradstein et al.* [1994] used to convert stratigraphic ages to absolute ages.

[c]Parentheses in Approximate Timing indicate minor phases of deformation or magmatic events. The ages not in parentheses indicate the major phase of deformation, or period of most voluminous magmatism, while ages within parentheses indicate periods of minor deformation or less voluminous magmatic emplacement.

rates (magnitude <2 cm/yr). The correlation coefficient for contraction events that developed contemporaneous with high convergence rates is 0.21 but increases to 0.32 if the Magallanes fold and thrust belt is excluded from the analysis.

5. Discussion

[26] Temporal and spatial associations between geological events and the plate parameters outlined above beg explanatory geodynamic mechanisms. In a global context, subduction zone polarity appears to be a strong determinant in the likelihood of developing back-arc basins, with most marginal basins being developed over west dipping subduction zones [*Dickinson*, 1978; *Doglioni*, 1995; *Doglioni et al.*, 2007]. The marginal basins of the Andean margin are thus part of a rarer group of back-arc basins developed along east dipping subduction zones and likely required the presence of unique conditions along the subduction zone to enable formation. The opening of mafic-floored back-arc basins along the South American margin was clearly associated with the trench normal absolute velocity vector being directed away from the trench. This conclusion agrees with the findings of other studies, which have indicated that absolute overriding plate velocity is a primary control on the tectonic regime of convergent margins [*Heuret and Lallemand*, 2005; *Oncken et al.*, 2006; *Ramos*, 2010]. Although overriding plate velocity alone has been suggested as a dominant factor on upper plate deformation [*Heuret and Lallemand*, 2005], other studies suggest that the differential velocity between the overriding plate and the trench is a stronger determinant of upper plate strain [*Oncken et al.*, 2006; *Ramos*, 2010]. As the plate model used does not currently incorporate trench motions, this study did not quantitatively consider this differential velocity as a parameter; however, trench velocity is considered to be itself dependent on the overriding plate velocity [*Oncken et al.*, 2006; *Ramos*, 2010], and so the first-order correlation observed with the overriding plate velocity agrees with these studies.

[27] Alone, the effect of the overriding plate velocity directed away from the trench appears inadequate to facilitate crustal separation and, for example, microcontinent dispersal. The development of back-arc basins in the northern and southern Andes regions was associated with the subduction of oceanic slabs older than 50 Myr. The effect of slab age on subduction dynamics is ambiguous. The buoyancy (age, thermal regime), rigidity, and the extent of coupling with the overriding plate, together with other parameters, have been shown to have a dependency on slab age yet are also considered to have distinct, commonly competing effects [*Forsyth and Uyeda*, 1975; *Di Giuseppe et al.*, 2009; *Yáñez and Cembrano*, 2004].

[28] Trench rollback, whereby the subduction zone hinge moves away from the overriding plate, is likely an important condition in the development of mafic-floored back-arc basins [*Oncken et al.*, 2006; *Ramos*, 2010]. However, as the model used in this analysis does not incorporate deformation of the trench, it cannot be used to provide a record of rollback along the margin. Slab age is sometimes employed as a proxy for trench rollback as rollback is commonly considered a consequence of the subduction of old, dense oceanic crust; younger slabs are commonly considered comparatively buoyant and thus able to resist subduction leading to trench advance [*Molnar and Atwater*, 1978; *Dewey*, 1980; *Garfunkel et al.*, 1986].

This could present a tidy explanation for the opening of mafic-floored back-arc basins facilitated by slab retreat from the subduction of old oceanic crust. However, in recent years the accepted relationship between slab age and trench movement has been challenged. A global compilation of absolute motions established the inverse relationship: older slabs advance toward the overriding plate and younger ones retreat [*Heuret and Lallemand*, 2005]. Older, stronger oceanic lithosphere supposedly resists bending at the subduction zone, resulting in trench advance, whereas younger, weaker crust subducts more easily resulting in trench retreat [*Di Giuseppe et al.*, 2009]. Instead of trench rollback, a potential first-order explanation for the correlation could be suction force, being derivative from the effect of subducted lithosphere displacing mantle material, in turn causing the overriding continental plate to be pulled toward the trench [*Elsasser*, 1971; *Forsyth and Uyeda*, 1975]. As older oceanic lithosphere tends to be thicker [*Parsons and McKenzie*, 1978], the subduction of relatively old oceanic lithosphere should displace proportionately more mantle material, inducing a stronger suction force than in the case of the subduction of younger lithosphere. In situations where the velocity of the overriding plate is negative, the tensile stress in the back-arc region can be envisaged as sufficient to induce crustal splitting, provided a preexisting weakness is present [*Shemenda*, 1993].

[29] An alternative explanation for the development of mafic-floored back-arc basins at only the northern and southernmost extents of the subduction margin involves a model whereby lateral slab width controls deformation in the overriding plate [*Schellart et al.*, 2007; *Schellart*, 2008]. In this model, mantle flow around the edges of a subducting slab enables rollback, facilitating lithospheric extension more easily at the edges of long subduction zones. Conversely, the lack of mantle escape flow in central portions of a subduction zone retards trench rollback. This effect may also explain why the development of mafic-floored back-arc basins does not occur at some other locations along the margin where the conditions of a negative overriding plate velocity and subducting slab age greater than 50 Myr are met (e.g., Point 49, Figures 3 and 4). However, location along the subduction zone cannot control the timing of the development of extension, and under this alternative model, the direction of the velocity of the overriding plate still seems to be a primary control on the initiation of mafic-floored back-arc basin extension.

[30] Modeled trench normal convergence rates less than 0 cm/yr (i.e., extensional) were associated with the opening of the Colombian Marginal Seaway (northern Andes) and the southern portion of the Rocas Verdes Basin (southern Andes). However, this condition does not appear essential to the development mafic-floored basins, as it was not associated with the opening of the northern portion of the Rocas Verdes Basin. Geological complexity of the Rocas Verdes Basin confounds easy interpretations. Geochemical distinctions between mafic rocks in southern and northern portions of the basin indicate that the basin was wider in the south than in the north, originally leading to an interpretation that crustal separation initiated in the south and propagated northward [*de Wit and Stern*, 1981; *Stern and de Wit*, 2003]. However, recent detrital zircon spectra from Rocas Verdes sedimentary rocks are more consistent with synchronous rifting along the length of the basin [*McAtamney et al.*, 2011], requiring an alternative explanation for distinctions between the southern

and northern mafic rocks. Convergence rates less than 0 cm/yr in the south but not in the north could have facilitated greater extension in the south and could explain the differences in basin width.

[31] The development of fold and thrust belts and plateau uplift along the South American margin, features commonly associated with crustal compression, seems to require contributing effects from parameters additional to those investigated here. Trench normal convergence velocity in excess of 4 cm/yr was correlated with the development of most contractional features, excluding the Magallanes fold and thrust belt. A high convergence rate could reasonably be expected to facilitate a compressive strain regime in the overriding continental plate, assuming regular plate coupling. However, convergence rates along the margin have been as high or higher during periods of extensional deformation or no contractional deformation (Figure 5). Therefore, while high convergence rates may facilitate the development of fold and thrust belts and plateau uplift, in isolation from other conditions, they are insufficient to drive overriding plate contraction. The age of the subducting slab has been suggested to have influenced the rise of the Andes, as the age of the Nazca Plate, with the oldest crust subducting in the center of the margin, correlates well with height and crustal thickening along the Andean margin [*Capitanio et al.*, 2011; *Yáñez and Cembrano*, 2004]. However, when the effect of slab age was examined in this analysis, it was found that correlation coefficients decreased slightly from 0.21 for convergence rate alone to 0.20 for combined convergence rate and slab age. The effect was slightly larger when the Magallanes fold and thrust belt was excluded from the analysis; the coefficients decreased from 0.32 to 0.30 for convergence rate alone and combined convergence rate and slab age, respectively. The subduction of slabs older than 50 Myr is largely absent from the development of fold and thrust belts in the Peruvian and south-central Andes, especially during the early episodes of thrusting in the Agrio and Aluminé fold and thrust belts (Figure 3). Clearly, if subducting slab age does play a role in contractional deformation in the overriding plate, it is not straightforward. It should also be noted that although the trench normal absolute velocity of South America is low in magnitude during these compression events, it is still positive, potentially contributing to the compressive regime.

[32] The Magallanes fold and thrust belt of the southern Andes presents an exception to the correlations established from other fold and thrust belts along the South American margin. Its development was accompanied by low trench normal convergence velocity: always less than 4 cm/yr and occasionally negative (tensional). The most probable causes of this inconsistency involve simplifications made in investigating the subduction parameters, namely that both internal deformation of South America and any change in trench geometry were disregarded. The portion of the South American Plate now in the southernmost Andes experienced shortening sufficient to bury components to circa 10–12 kbar [*Klepeis et al.*, 2010; *Maloney et al.*, 2011], but the global plate model used currently has no mechanism to incorporate the effects of such shortening on the geometry of a plate. The Patagonian Orocline initiated during or has become more pronounced since the mid-Cretaceous [e.g., *Kraemer*, 2003] resulting in changes in the shape of the margin that should influence plate velocities at relevant parts of the trench.

[33] An essential point to recall when interpreting these results is that correlations highlighted by this analysis do not necessarily imply causal relationships. Geodynamic mechanisms outlined above indicate that potential causal relationships may exist, but are not required by the results. In cases where the proposed mechanism agrees with results of previous studies, such as the tectonic control provided by the direction of overriding plate motion, the likelihood of the existence of a causal relationship is high.

[34] Several noncorrelations are additionally notable, as they allow parameters modeled in this study to be discounted as the primary drivers of a given geological event. For instance, periods inferred to have been accompanied by a high magmatic flux do not seem to correlate with any of the investigated parameters, either singly or in combination. Thus, it is inferred that high recorded rates of magmatic flux were not controlled by any of subducting slab age, absolute overriding plate velocity, or convergence velocity. In addition, the subduction of spreading ridges, commonly invoked as a cause of orogenesis initiation [*Palmer*, 1968; *Ramos*, 2005], has no correlation with any type of deformation and thus appears to have had a negligible effect on foreland deformation along the Andean margin (Figures 3–5). This study also separated structural styles of fold and thrust belts but failed to determine any correlation between any of the modeled subduction parameters and the development of thin- or thick-skinned thrusting. The reactivation of Mesozoic extensional structures to form thick-skinned fold and thrust belts is common along the margin, recorded in the Eastern Cordillera of Colombia, the Santa Bárbara System, and various thrust belts of the Neuquén Basin [*Parra et al.*, 2009a, 2009b; *Reynolds et al.*, 2000; *Grier et al.*, 1991; *Giambiagi et al.*, 2008; *Ramos et al.*, 1996; *Zapata and Folguera*, 2005; *Folguera et al.*, 2007; *García Morabito et al.*, 2011]. However, earlier Mesozoic deformation does not appear to be uniquely deterministic of contractional deformation style. For instance, during the middle to Late Cretaceous episode of thrusting, the Chos Malal fold and thrust belt developed a thin-skinned style due to the availability of detachment surfaces despite the presence of earlier extensional features which were reactivated in the second deformation episode of the belt [*Folguera et al.*, 2007]. In contrast with *Kley et al.* [1999], rather than being dominantly controlled by inherited Mesozoic extensional structures, thrusting style appears to be the result of the interplay of various factors including Mesozoic deformation, contrasts between differing lithologies or sediment thickness, and the orientation of preexisting structures.

[35] This investigation focused on the relationships between geology and the forces acting at the subduction zone at the boundary of the interacting plates, but forces acting internally on the overriding plate have been omitted as a quantitative assessment of these forces would be beyond the scope of this study. Thickening or thinning of the lithosphere in response to subduction along the margin can introduce lateral contrasts in the gravitational potential energy of a region which results in ductile flow of the lithosphere to reduce those contrasts [*Rey et al.*, 2001]. Therefore, gravitational forces can lead to deformation independent of the subduction zone parameters and may be a factor in some of the observed discrepancies.

13

[36] This investigation has assumed that the kinematic model used to determine the subduction-related parameters accurately represents conditions along the margin back to 170 Ma. However, there can be significant variations between models, particularly at older times. The method outlined in this paper could easily be adapted to test several different models to determine which best reproduces the major geological events in the overriding plate. Such a test could determine whether the observed correlations are robust across the models or potential artefacts of specific models.

6. Conclusions

[37] The examination of the Andean margin over the past 170 Ma has allowed for the determination of the conditions imposed by the subduction zone necessary for the development of geological events in the overriding plate. Key findings include the following:

[38] 1. Continental extension may reflect a series of distinct conditions for which no correlation could be established. Nonetheless, extension that progresses to forming new oceanic crust requires that the trench normal absolute velocity of the overriding plate be directed away from the trench *and* that the age of the subducting slab be older than 50 Myr.

[39] 2. Plateau uplift and the development of fold and thrust belts generally developed in the presence of trench normal convergence velocities greater than 4 cm/yr.

[40] 3. Trench normal convergence velocities greater than 4 cm/yr prior to the development of contractional features indicate that while high convergence velocities may facilitate shortening of the overriding crust, other conditions are necessary for the initiation of contraction.

[41] 4. The direction of the motion of the overriding plate appears to control the overall tectonic regime.

[42] 5. No correlations could be established between the modeled subduction parameters investigated and major magmatic events, or with the structural style developed in fold and thrust belts.

[43] 6. Spreading ridge impingement on the margin was uncorrelated with the initiation of orogenesis.

References

Allmendinger, R. W., T. E. Jordan, S. M. Kay, and B. L. Isacks (1997), The evolution of the Altiplano-Puna plateau of the Central Andes, *Annu. Rev. Earth Planet. Sci.*, *25*(1), 139–174, doi:10.1146/annurev.earth.25.1.139.

Aspden, J. A., and W. J. McCourt (1986), Mesozoic oceanic terrane in the central Andes of Colombia, *Geology*, *14*(5), 415–418, doi:10.1130/0091-7613(1986)14<415:MOTITC>2.0.CO;2.

Atherton, M. P., and L. Aguirre (1992), Thermal and geotectonic setting of Cretaceous volcanic rocks near Ica, Peru, in relation to Andean crustal thinning, *J. S. Am. Earth Sci.*, *5*(1), 47–69, doi:10.1016/0895-9811(92)90059-8.

Atherton, M. P., and N. Petford (1996), Plutonism and the growth of Andean Crust at 9°S from 100 to 3 Ma, *J. S. Am. Earth Sci.*, *9*(1-2), 1–9, doi:10.1016/0895-9811(96)00023-5.

Atherton, M. P., W. S. Pitcher, and V. Warden (1983), The Mesozoic marginal basin of central Peru, *Nature*, *305*(5932), 303–306, doi:10.1038/305303a0.

Audebaud, E., R. Capdevila, B. Dalmayrac, J. Debelmas, G. Laubacher, C. Lefèvre, R. Marocco, C. Martinez, M. Mattauer, and F. Mégard (1973), Les traits géologiques essentiels des Andes centrales (Pérou-Bolivie), *Rev. Géogr. Phys. Géol. Dyn.*, *15*(1-2), 73–114.

Barazangi, M., and B. L. Isacks (1976), Spatial distribution of earthquakes and subduction of the Nazca plate beneath South America, *Geology*, *4*(11), 686–692, doi:10.1130/0091-7613(1976)4<686:sdoeas>2.0.co;2.

Beck, S. L., and G. Zandt (2002), The nature of orogenic crust in the central Andes, *J. Geophys. Res.*, *107*(B10), 2230, doi:10.1029/2000jb000124.

Beck, S. L., G. Zandt, S. C. Myers, T. C. Wallace, P. G. Silver, and L. Drake (1996), Crustal-thickness variations in the central Andes, *Geology*, *24*(5), 407–410, doi:10.1130/0091-7613(1996)024<0407:ctvitc>2.3.co;2.

Bruhn, R. L., C. R. Stern, and M. J. De Wit (1978), Field and geochemical data bearing on the development of a Mesozoic volcano-tectonic rift zone and back-arc basin in southernmost South America, *Earth Planet. Sci. Lett.*, *41*(1), 32–46, doi:10.1016/0012-821X(78)90039-0.

Burchfiel, B. C., P. Molnar, and G. Suaréz (1981), Possible think-skin tectonics in the eastern Andes of Bolivia and Peru (abstract), *Eos Trans. AGU*, *62*(45), 1047, doi:10.1029/EO062i045p00794.

Burns, W. (2002), Tectonics of the Southern Andes from stratigraphic, thermochronologic, and geochemical perspectives, Ph.D. thesis, Cornell University, Ithaca, New York.

Burns, W. M., T. E. Jordan, P. Copeland, and S. A. Kelley (2006), The case for extensional tectonics in the Oligocene-Miocene Southern Andes as recorded in the Cura Mallín basin (36°–38°S), *Geol. Soc. Am. Spec. Pap.*, *407*, 163–184, doi:10.1130/2006.2407(08).

Calderón, M., A. Fildani, F. Hervé, C. M. Fanning, A. Weislogel, and U. Cordani (2007), Late Jurassic bimodal magmatism in the northern sea-floor remnant of the Rocas Verdes basin, southern Patagonian Andes, *J. Geol. Soc. London*, *164*(5), 1011–1022, doi:10.1144/0016-76492006-102.

Capitanio, F. A., C. Faccenna, S. Zlotnik, and D. R. Stegman (2011), Subduction dynamics and the origin of Andean orogeny and the Bolivian orocline, *Nature*, *480*(7375), 83–86, doi:10.1038/nature10596.

Carrera, N., J. A. Muñoz, F. Sàbat, R. Mon, and E. Roca (2006), The role of inversion tectonics in the structure of the Cordillera Oriental (NW Argentinean Andes), *J. Struct. Geol.*, *28*(11), 1921–1932, doi:10.1016/j.jsg.2006.07.006.

Charrier, R., O. Baeza, S. Elgueta, J. J. Flynn, P. Gans, S. M. Kay, N. Muñoz, A. R. Wyss, and E. Zurita (2002), Evidence for Cenozoic extensional basin development and tectonic inversion south of the flat-slab segment, southern Central Andes, Chile (33°–36°S.L.), *J. S. Am. Earth Sci.*, *15*(1), 117–139, doi:10.1016/S0895-9811(02)00009-3.

Cobbing, E. J. (1978), The Andean geosyncline in Peru, and its distinction from Alpine geosynclines, *J. Geol. Soc. London*, *135*(2), 207–218, doi:10.1144/gsjgs.135.2.0207.

Coira, B., J. Davidson, C. Mpodozis, and V. Ramos (1982), Tectonic and magmatic evolution of the Andes of northern Argentina and Chile, *Earth Sci. Rev.*, *18*(3-4), 303–332, doi:10.1016/0012-8252(82)90042-3.

Cristallini, E. O., and V. A. Ramos (2000), Thick-skinned and thin-skinned thrusting in the La Ramada fold and thrust belt: Crustal evolution of the High Andes of San Juan, Argentina (32°SL), *Tectonophysics*, *317*(3-4), 205–235, doi:10.1016/S0040-1951(99)00276-0.

Cunningham, W. D. (1993), Strike-slip faults in the southernmost Andes and the development of the Patagonian orocline, *Tectonics*, *12*(1), 169–186, doi:10.1029/92tc01790.

Cunningham, W. D., K. A. Klepeis, W. A. Gose, and I. W. D. Dalziel (1991), The Patagonian Orocline: New paleomagnetic data from the Andean magmatic arc in Tierra del Fuego, Chile, *J. Geophys. Res.*, *96*(B10), 16,061–16,067, doi:10.1029/91JB01498.

Daly, M. C. (1989), Correlations between Nazca/Farallon Plate kinematics and forearc basin evolution in Ecuador, *Tectonics*, *8*(4), 769–790, doi:10.1029/TC008i004p00769.

Dalziel, I. W. D., M. J. De Wit, and K. F. Palmer (1974), Fossil marginal basin in the southern Andes, *Nature*, *250*(5464), 291–294, doi:10.1038/250291a0.

Dewey, J. F. (1980), Episodicity, sequence and style at convergent plate boundaries, in *The Continental Crust and Its Mineral Deposits*, edited by D. W. Strangway, *Geol. Assoc. Can. Spec. Pap.*, *20*, 553–573.

de Wit, M. J., and C. R. Stern (1981), Variations in the degree of crustal extension during formation of a back-arc basin, *Tectonophysics*, *72*, 229–260, doi:10.1016/0040-1951(81)90240-7.

Di Giuseppe, E., C. Faccenna, F. Funiciello, J. van Hunen, and D. Giardini (2009), On the relation between trench migration, seafloor age, and the strength of the subducting lithosphere, *Lithosphere*, *1*(2), 121–128, doi:10.1130/l26.1.

Dickinson, W. R. (1978), Plate tectonic evolution of North Pacific rim, *J. Phys. Earth*, *26*, 1–19.

Doglioni, C. (1995), Geological remarks on the relationships between extension and convergent geodynamic settings, *Tectonophysics*, *252*(1–4), 253–267, doi:10.1016/0040-1951(95)00087-9.

Doglioni, C., E. Carminati, M. Cuffaro, and D. Scrocca (2007), Subduction kinematics and dynamic constraints, *Earth Sci. Rev.*, *83*(3–4), 125–175, doi:10.1016/j.earscirev.2007.04.001.

Elsasser, W. M. (1971), Sea-floor spreading as thermal convection, *J. Geophys. Res.*, *76*(5), 1101–1112, doi:10.1029/JB076i005p01101.

Fildani, A., and A. M. Hessler (2005), Stratigraphic record across a retroarc basin inversion: Rocas Verdes-Magallanes Basin, Patagonian Andes, Chile, *Geol. Soc. Am. Bull.*, *117*(11-12), 1596–1614, doi:10.1130/B25708.1.

Fildani, A., T. D. Cope, S. A. Graham, and J. L. Wooden (2003), Initiation of the Magallanes foreland basin: Timing of the southernmost Patagonian Andes orogeny revised by detrital zircon provenance analysis, *Geology*, *31*(12), 1081–1084, doi:10.1130/g20016.1.

Folguera, A., V. A. Ramos, E. F. González Díaz, and R. Hermanns (2006), Miocene to Quaternary deformation of the Guañacos fold-and-thrust belt in the Neuquén Andes between 37°S and 37°30′S, *Geol. Soc. Am. Spec. Pap.*, *407*, 247–266, doi:10.1130/2006.2407(11).

Folguera, A., V. A. Ramos, T. Zapata, and M. G. Spagnuolo (2007), Andean evolution at the Guañacos and Chos Malal fold and thrust belts (36°30′–37°s), *J. Geodyn.*, *44*(3–5), 129–148, doi:10.1016/j.jog.2007.02.003.

Forsyth, D., and S. Uyeda (1975), On the relative importance of the driving forces of plate motion, *Geophys. J. R. Astron. Soc.*, *43*(1), 163–200, doi:10.1111/j.1365-246X.1975.tb00631.x.

Fosdick, J. C., B. W. Romans, A. Fildani, A. Bernhardt, M. Calderon, and S. A. Graham (2011), Kinematic evolution of the Patagonian retroarc fold-and-thrust belt and Magallanes foreland basin, Chile and Argentina, 51°30'S, *Geol. Soc. Am. Bull.*, *123*(9-10), 1679–1698, doi:10.1130/b30242.1.

Franzese, J. R., L. D'Elia, A. Bilmes, M. Muravchik, and M. Hernández (2011), Superposición de cuencas extensionales y contraccionales oligo-miocenas en el retroarco andino norpatagónico: la Cuenca de Aluminé, Neuquén, Argentina, *Andean Geol.*, *38*(2), 319–334.

García Morabito, E., and V. A. Ramos (2012), Andean evolution of the Aluminé fold and thrust belt, Northern Patagonian Andes (38°30′–40°30′S), *J. S. Am. Earth Sci.*, *38*, 13–30, doi:10.1016/j.jsames.2012.03.005.

García Morabito, E., H.-J. Götze, and V. A. Ramos (2011), Tertiary tectonics of the Patagonian Andes retro-arc area between 38°15′ and 40°S latitude, *Tectonophysics*, *499*(1–4), 1–21, doi:10.1016/j.tecto.2010.10.020.

Garfunkel, Z., C. A. Anderson, and G. Schubert (1986), Mantle circulation and the lateral migration of subducted slabs, *J. Geophys. Res.*, *91*(B7), 7205–7223, doi:10.1029/JB091iB07p07205.

Gerbault, M., J. Martinod, and G. Hérail (2005), Possible orogeny-parallel lower crustal flow and thickening in the Central Andes, *Tectonophysics*, *399*, 59–72, doi:10.1016/j.tecto.2004.12.015.

Ghidella, M. A., G. Yáñez, and J. L. LaBrecque (2002), Revised tectonic implications for the magnetic anomalies of the western Weddell Sea, *Tectonophysics*, *347*, 65–86, doi:10.1016/S0040-1951(01)00238-4.

Giacosa, R. E., J. C. Afonso, N. Heredia C, and J. Paredes (2005), Tertiary tectonics of the sub-Andean region of the North Patagonian Andes, southern central Andes of Argentina (41–42°30′S), *J. S. Am. Earth Sci.*, *20*(3), 157–170, doi:10.1016/j.jsames.2005.05.013.

Giambiagi, L., F. Bechis, V. García, and A. H. Clark (2008), Temporal and spatial relationships of thick- and thin-skinned deformation: A case study from the Malargüe fold-and-thrust belt, southern Central Andes, *Tectonophysics*, *459*(1-4), 123–139, doi:10.1016/j.tecto.2007.11.069.

Giovanni, M. K., B. K. Horton, C. N. Garzione, B. McNulty, and M. Grove (2010), Extensional basin evolution in the Cordillera Blanca, Peru: Stratigraphic and isotopic records of detachment faulting and orogenic collapse in the Andean hinterland, *Tectonics*, *29*, TC6007, doi:10.1029/2010tc002666.

Godoy, E., G. Yañez, and E. Vera (1999), Inversion of an Oligocene volcano-tectonic basin and uplifting of its superimposed Miocene magmatic arc in the Chilean Central Andes: First seismic and gravity evidences, *Tectonophysics*, *306*(2), 217–236, doi:10.1016/S0040-1951(99)00046-3.

Gradstein, F. M., F. P. Agterberg, J. G. Ogg, J. Hardenbol, P. van Veen, J. Thierry, and Z. Huang (1994), A Mesozoic time scale, *J. Geophys. Res.*, *99*(B12), 24,051–24,074, doi:10.1029/94jb01889.

Grier, M. E., J. A. Salfity, and R. W. Allmendinger (1991), Andean reactivation of the Cretaceous Salta rift, northwestern Argentina, *J. S. Am. Earth Sci.*, *4*(4), 351–372, doi:10.1016/0895-9811(91)90007-8.

Gubbels, T. L., B. L. Isacks, and E. Farrar (1993), High-level surfaces, plateau uplift, and foreland development, Bolivian central Andes, *Geology*, *21*(8), 695–698, doi:10.1130/0091-7613(1993)021<0695:hlspua>2.3.co;2.

Halpern, M. (1973), Regional geochronology of Chile south of 50° latitude, *Geol. Soc. Am. Bull.*, *84*(7), 2407–2422, doi:10.1130/0016-7606(1973)84<2407:RGOCSO>2.0.CO;2.

Hervé, M., M. Suárez, and A. Puig (1984), The Patagonian Batholith S of Tierra del Fuego, Chile: Timing and tectonic implications, *J. Geol. Soc. London*, *141*(5), 909–917, doi:10.1144/gsjgs.141.5.0909.

Hervé, F., H. Miller, and C. Pimpirev (2006), Patagonia—Antarctic connections before Gondwana break-up, in *Antarctica: Contributions to Global Earth Sciences*, edited by D. Futterer et al., pp. 217–228, Springer, Berlin.

Hervé, F., R. J. Pankhurst, C. M. Fanning, M. Calderón, and G. M. Yaxley (2007), The South Patagonian batholith: 150 my of granite magmatism on a plate margin, *Lithos*, *97*(3-4), 373–394, doi:10.1016/j.lithos.2007.01.007.

Heuret, A., and S. Lallemand (2005), Plate motions, slab dynamics and back-arc deformation, *Phys. Earth Planet. Inter.*, *149*(1-2), 31–51, doi:10.1016/j.pepi.2004.08.022.

Isacks, B. L. (1988), Uplift of the Central Andean Plateau and bending of the Bolivian Orocline, *J. Geophys. Res.*, *93*(B4), 3211–3231, doi:10.1029/JB093iB04p03211.

Jaillard, E., T. Sempere, P. Soler, G. Carlier, and R. Marocco (1995), The role of Tethys in the evolution of the Northern Andes between Late Permian and Late Eocene times, in *Ocean Basins and Margins*, vol. 8, *The Tethys Ocean*, edited by A. E. M. Nairn et al., pp. 463–492, Plenum, New York.

James, D. E. (1971), Plate tectonic model for the evolution of the central Andes, *Geol. Soc. Am. Bull.*, *82*(12), 3325–3346, doi:10.1130/0016-7606(1971)82[3325:ptmfte]2.0.co;2.

Jarrard, R. D. (1986), Relations among subduction parameters, *Rev. Geophys.*, *24*(2), 217–284, doi:10.1029/RG024i002p00217.

Jokat, W., T. Boebel, M. König, and U. Meyer (2003), Timing and geometry of early Gondwana breakup, *J. Geophys. Res.*, *108*(B9), 2428, doi:10.1029/2002jb001802.

Jordan, T., R. Allmendinger, J. Damanti, and R. Drake (1993), Chronology of motion in a complete thrust belt: The Precordillera, 30–31°S, Andes Mountains, *J. Geol.*, *101*(2), 135–156.

Jordan, T. E., W. M. Burns, R. Veiga, F. Pángaro, P. Copeland, S. Kelley, and C. Mpodozis (2001), Extension and basin formation in the southern Andes caused by increased convergence rate: A mid-Cenozoic trigger for the Andes, *Tectonics*, *20*(3), 308–324, doi:10.1029/1999tc001181.

Kay, S. M., W. M. Burns, P. Copeland, and O. Mancilla (2006), Upper Cretaceous to Holocene magmatism and evidence for transient Miocene shallowing of the Andean subduction zone under the northern Neuquén Basin, *Geol. Soc. Am. Spec. Pap.*, *407*, 19–60, doi:10.1130/2006.2407(02).

Kennan, L., and J. L. Pindell (2009), Dextral shear, terrane accretion and basin formation in the Northern Andes: Best explained by interaction with a Pacific-derived Caribbean Plate?, *Geol. Soc. Spec. Publ.*, *328*(1), 487–531, doi:10.1144/sp328.20.

Klepeis, K. A. (1994), The Magallanes and Deseado fault zones: Major segments of the South American-Scotia transform plate boundary in southernmost South America, Tierra del Fuego, *J. Geophys. Res.*, *99*(B11), 22,001–22,014, doi:10.1029/94JB01749.

Klepeis, K. A., and J. A. Austin (1997), Contrasting styles of superposed deformation in the southernmost Andes, *Tectonics*, *16*(5), 755–776, doi:10.1029/97TC01611.

Klepeis, K., P. Betka, G. Clarke, M. Fanning, F. Hervé, L. Rojas, C. Mpodozis, and S. Thomson (2010), Continental underthrusting and obduction during the Cretaceous closure of the Rocas Verdes rift basin, Cordillera Darwin, Patagonian Andes, *Tectonics*, *29*, TC3014, doi:10.1029/2009tc002610.

Kley, J., and C. R. Monaldi (2002), Tectonic inversion in the Santa Barbara System of the central Andean foreland thrust belt, northwestern Argentina, *Tectonics*, *21*(6), 1061, doi:10.1029/2002tc902003.

Kley, J., C. R. Monaldi, and J. A. Salfity (1999), Along-strike segmentation of the Andean foreland: Causes and consequences, *Tectonophysics*, *301*(1-2), 75–94, doi:10.1016/S0040-1951(98)90223-2.

Kozlowski, E., R. Manceda, and V. A. Ramos (1993), Estructura, in *Geología y Recursos Naturales de Mendoza*, paper presented at *XII Congreso Geológico Argentino y II Congreso Exploración de Hidrocarburos*, Buenos Aires.

Kraemer, P. (1998), Structure of the Patagonian Andes: Regional balanced cross section at 50°S, Argentina, *Int. Geol. Rev.*, *40*(10), 896–915, doi:10.1080/00206819809465244.

Kraemer, P. E. (2003), Orogenic shortening and the origin of the Patagonian orocline (56°S. Lat), *J. S. Am. Earth Sci.*, *15*(7), 731–748, doi:10.1016/S0895-9811(02)00132-3.

Lallemand, S., A. Heuret, and D. Boutelier (2005), On the relationships between slab dip, back-arc stress, upper plate absolute motion, and crustal nature in subduction zones, *Geochem. Geophys. Geosyst.*, *6*, Q09006, doi:10.1029/2005gc000917.

Lawver, L. A., L. M. Gahagan, and I. W. D. Dalziel (1998), A tight fit early Mesozoic Gondwana, a plate reconstruction perspective, *Natl. Inst. Polar Res. Spec. Issue*, *53*, 214–229.

Levi, B., and L. Aguirre (1981), Ensialic spreading-subsidence in the Mesozoic and Palaeogene Andes of central Chile, *J. Geol. Soc. London*, *138*(1), 75–81, doi:10.1144/gsjgs.138.1.0075.

Maloney, K. T., G. L. Clarke, K. A. Klepeis, C. M. Fanning, and W. Wang (2011), Crustal growth during back-arc closure: Cretaceous exhumation history of Cordillera Darwin, southern Patagonia, *J. Metamorph. Geol.*, *29*(6), 649–672, doi:10.1111/j.1525-1314.2011.00934.x.

Marquillas, R. A., C. del Papa, and I. F. Sabino (2005), Sedimentary aspects and paleoenvironmental evolution of a rift basin: Salta Group (Cretaceous-Paleogene), northwestern Argentina, *Int. J. Earth Sci.*, *94*(1), 94–113, doi:10.1007/s00531-004-0443-2.

Martinod, J., L. Husson, P. Roperch, B. Guillaume, and N. Espurt (2010), Horizontal subduction zones, convergence velocity and the building of the Andes, *Earth Planet. Sci. Lett.*, *299*(3-4), 299–309, doi:10.1016/j.epsl.2010.09.010.

McAtamney, J., K. Klepeis, C. Mehrtens, S. Thomson, P. Betka, L. Rojas, and S. Snyder (2011), Along-strike variability of back-arc basin collapse and the initiation of sedimentation in the Magallanes foreland basin, southernmost Andes (53–54.5°S), *Tectonics*, *30*, TC5001, doi:10.1029/2010tc002826.

McCourt, W. J., J. A. Apsden, and M. Brook (1984), New geological and geochronological data from the Colombian Andes: Continental growth by multiple accretion, *J. Geol. Soc. London*, *141*, 831–845, doi:10.1144/gsjgs.141.5.0831.

McNulty, B., and D. Farber (2002), Active detachment faulting above the Peruvian flat slab, *Geology*, *30*(6), 567–570, doi:10.1130/0091-7613 (2002)030<0567:adfatp>2.0.co;2.

McQuarrie, N., B. K. Horton, G. Zandt, S. Beck, and P. G. DeCelles (2005), Lithospheric evolution of the Andean fold-thrust belt, Bolivia, and the origin of the central Andean plateau, *Tectonophysics*, *399*(1-4), 15–37, doi:10.1016/j.tecto.2004.12.013.

Mégard, F. (1984), The Andean orogenic period and its major structures in central and northern Peru, *J. Geol. Soc. London*, *141*(5), 893–900, doi:10.1144/gsjgs.141.5.0893.

Molnar, P., and T. Atwater (1978), Interarc spreading and Cordilleran tectonics as alternates related to the age of subducted oceanic lithosphere, *Earth Planet. Sci. Lett.*, *41*(3), 330–340, doi:10.1016/0012-821x(78)90187-5.

Mora, A., T. Gaona, J. Kley, D. Montoya, M. Parra, L. I. Quiroz, G. Reyes, and M. R. Strecker (2009), The role of inherited extensional fault segmentation and linkage in contractional orogenesis: A reconstruction of Lower Cretaceous inverted rift basins in the Eastern Cordillera of Colombia, *Basin Res.*, *21*(1), 111–137, doi:10.1111/j.1365-2117.2008.00367.x.

Mpodozis, C., and R. W. Allmendinger (1993), Extensional tectonics, Cretaceous Andes, northern Chile (27°S), *Geol. Soc. Am. Bull.*, *105*(11), 1462–1477, doi:10.1130/0016-7606(1993)105<1462:etcanc>2.3.co;2.

Mukasa, S. B. (1986), Zircon U-Pb ages of super-units in the Coastal batholith, Peru: Implications for magmatic and tectonic processes, *Geol. Soc. Am. Bull.*, *97*(2), 241–254, doi:10.1130/0016-7606(1986)97<241:zuaosi>2.0.co;2.

Nelson, E. P., I. W. D. Dalziel, and A. G. Milnes (1980), Structural geology of the Cordillera Darwin - collisional-style orogenesis in the southernmost Chilean Andes, *Eclogae Geol. Helv.*, *73*, 727–751.

Nivia, A., G. F. Marriner, A. C. Kerr, and J. Tarney (2006), The Quebradagrande Complex: A Lower Cretaceous ensialic marginal basin in the Central Cordillera of the Colombian Andes, *J. S. Am. Earth Sci.*, *21*(4), 423–436, doi:10.1016/j.jsames.2006.07.002.

Oliveros, V., G. Féraud, L. Aguirre, M. Fornari, and D. Morata (2006), The Early Andean Magmatic Province (EAMP): 40Ar/39Ar dating on Mesozoic volcanic and plutonic rocks from the Coastal Cordillera, northern Chile, *J. Volcanol. Geotherm. Res.*, *157*(4), 311–330, doi:10.1016/j.jvolgeores.2006.04.007.

Oncken, O., D. Hindle, J. Kley, K. Elger, P. Victor, and K. Schemmann (2006), Deformation of the Central Andean upper plate system—Facts, fiction, and constraints for plateau models, in *The Andes*, edited by O. Oncken et al., pp. 3–27, Springer, Berlin.

O'Neill, C., D. Müller, and B. Steinberger (2005), On the uncertainties in hot spot reconstructions and the significance of moving hot spot reference frames, *Geochem. Geophys. Geosyst.*, *6*, Q04003, doi:10.1029/2004gc000784.

Palmer, H. (1968), East Pacific Rise and westward drift of North America, *Nature*, *220*(5165), 341–345, doi:10.1038/220341a0.

Pankhurst, R. J., S. D. Weaver, F. Hervé, and P. Larrondo (1999), Mesozoic-Cenozoic evolution of the North Patagonian Batholith in Aysén, southern Chile, *J. Geol. Soc. London*, *156*(4), 673–694, doi:10.1144/gsjgs.156.4.0673.

Pankhurst, R. J., T. R. Riley, C. M. Fanning, and S. P. Kelley (2000), Episodic silicic volcanism in Patagonia and the Antarctic Peninsula: Chronology of magmatism associated with the break-up of Gondwana, *J. Petrol.*, *41*(5), 605–625, doi:10.1093/petrology/41.5.605.

Paredes, J. M., R. E. Giacosa, and N. Heredia (2009), Sedimentary evolution of Neogene continental deposits (Ñirihuau Formation) along the Ñirihuau River, North Patagonian Andes of Argentina, *J. S. Am. Earth Sci.*, *28*(1), 74–88, doi:10.1016/j.jsames.2009.01.002.

Parra, M., A. Mora, C. Jaramillo, M. R. Strecker, E. R. Sobel, L. Quiroz, M. Rueda, and V. Torres (2009a), Orogenic wedge advance in the northern Andes: Evidence from the Oligocene-Miocene sedimentary record of the Medina Basin, Eastern Cordillera, Colombia, *Geol. Soc. Am. Bull.*, *121*(5-6), 780–800, doi:10.1130/b26257.1.

Parra, M., A. Mora, E. R. Sobel, M. R. Strecker, and R. González (2009b), Episodic orogenic front migration in the northern Andes: Constraints from low-temperature thermochronology in the Eastern Cordillera, Colombia, *Tectonics*, *28*, TC4004, doi:10.1029/2008tc002423.

Parra, M., A. Mora, C. Lopez, L. Ernesto Rojas, and B. K. Horton (2012), Detecting earliest shortening and deformation advance in thrust belt hinterlands: Example from the Colombian Andes, *Geology*, *40*(2), 175–178, doi:10.1130/g32519.1.

Parsons, B., and D. McKenzie (1978), Mantle convection and the thermal structure of the plates, *J. Geophys. Res.*, *83*(B9), 4485–4496, doi:10.1029/JB083iB09p04485.

Pilger, R. H. (1981), Plate reconstructions, aseismic ridges, and low-angle subduction beneath the Andes, *Geol. Soc. Am. Bull.*, *92*(7), 448–456, doi:10.1130/0016-7606(1981)92<448:praral>2.0.co;2.

Pilger, R. H. (1984), Cenozoic plate kinematics, subduction and magmatism: South American Andes, *J. Geol. Soc. London*, *141*(5), 793–802, doi:10.1144/gsjgs.141.5.0793.

Pindell, J., and J. F. Dewey (1982), Permo-Triassic reconstruction of western Pangea and the evolution of the Gulf of Mexico/Caribbean region, *Tectonics*, *1*(2), 179–211, doi:10.1029/TC001i002p00179.

Pindell, J. L., and L. Kennan (2009), Tectonic evolution of the Gulf of Mexico, Caribbean and northern South America in the mantle reference frame: An update, *Geol. Soc. Spec. Publ.*, *328*(1), 1–55, doi:10.1144/sp328.1.

Pindell, J. L., and K. Tabbutt (1995), Mesozoic-Cenozoic Andean paleogeography and regional controls on hydrocarbon systems, in *Petroleum Basins of South America*, edited by A. J. Tankard, R. Suarez, and H. J. Welsink, *AAPG Mem.*, *62*, 101–128.

Ramos, V. A. (1985), El Mesozoico de la Alta Codillera de Mendoza: Reconstrussion tectónica de sus facies, Argentina, *Antofagasta, IV Congr. Geol. Chileno Actas*, *1*, 491–513.

Ramos, V. A. (2005), Seismic ridge subduction and topography: Foreland deformation in the Patagonian Andes, *Tectonophysics*, *399*(1-4), 73–86, doi:10.1016/j.tecto.2004.12.016.

Ramos, V. A. (2010), The tectonic regime along the Andes: Present-day and Mesozoic regimes, *Geol. J.*, *45*(1), 2–25, doi:10.1002/gj.1193.

Ramos, V. A., and S. M. Kay (2006), Overview of the tectonic evolution of the southern Central Andes of Mendoza and Neuquén (35°–39°S latitude), *Geol. Soc. Am. Spec. Pap.*, *407*, 1–17, doi:10.1130/2006.2407(01).

Ramos, V. A., M. Cegarra, and E. Cristallini (1996), Cenozoic tectonics of the High Andes of west-central Argentina (30–36°S latitude), *Tectonophysics*, *259*(1-3), 185–200, doi:10.1016/0040-1951(95)00064-X.

Ramos, V. A., E. O. Cristallini, and D. J. Pérez (2002), The Pampean flat-slab of the Central Andes, *J. S. Am. Earth Sci.*, *15*(1), 59–78, doi:10.1016/S0895-9811(02)00006-8.

Rapela, C. W., L. A. Spalletti, and J. Merodio (1983), Evolución magmática y geotectónica de la Serie Andesítica Andina (PaleocenoEoceno) en la Cordillera Norpatagónica, *Rev. Asoc. Geol. Argent.*, *38*(3-4), 469–484.

Rey, P., O. Vanderhaeghe, and C. Teyssier (2001), Gravitational collapse of the continental crust: Definition, regimes and modes, *Tectonophysics*, *342*(3-4), 435–449, doi:10.1016/S0040-1951(01)00174-3.

Reyes, F. C. (1972), Correlaciones en el Cretácico de la cuenca Andina de Bolivia, Peru y Chile, *Rev. Téc. Yacimientos Pet. Fiscales Boliv.*, *1*, 101–144.

Reynolds, J. H., C. I. Galli, R. M. Hernandez, B. D. Idleman, J. M. Kotila, R. V. Hilliard, and C. W. Naeser (2000), Middle Miocene tectonic development of the Transition Zone, Salta Province, northwest Argentina: Magnetic stratigraphy from the Metan Subgroup, Sierra de Gonzalez, *Geol. Soc. Am. Bull.*, *112*(11), 1736–1751, doi:10.1130/0016-7606(2000)112<1736:mmtdot>2.0.co;2.

Rosenau, M., D. Melnick, and H. Echtler (2006), Kinematic constraints on intra-arc shear and strain partitioning in the southern Andes between 38°S and 42°S latitude, *Tectonics*, *25*, TC4013, doi:10.1029/2005tc001943.

Ross, M. I., and C. R. Scotese (1988), A hierarchical tectonic model of the Gulf of Mexico and Caribbean region, *Tectonophysics*, *155*(1–4), 139–168, doi:10.1016/0040-1951(88)90263-6.

Rousse, S., S. Gilder, D. Farber, B. McNulty, P. Patriat, V. Torres, and T. Sempere (2003), Paleomagnetic tracking of mountain building in the Peruvian Andes since 10 Ma, *Tectonics*, *22*(5), 1048, doi:10.1029/2003tc001508.

Schellart, W. P. (2008), Overriding plate shortening and extension above subduction zones: A parametric study to explain formation of the Andes Mountains, *Geol. Soc. Am. Bull.*, *120*(11-12), 1441–1454, doi:10.1130/b26360.1.

Schellart, W. P., J. Freeman, D. R. Stegman, L. Moresi, and D. May (2007), Evolution and diversity of subduction zones controlled by slab width, *Nature*, *446*, 308–311, doi:10.1038/nature05615.

Seton, M., et al. (2012), Global continental and ocean basin reconstructions since 200 Ma, *Earth Sci. Rev.*, *113*(3–4), 212–270, doi:10.1016/j.earscirev.2012.03.002.

Shemenda, A. I. (1993), Subduction of the lithosphere and back arc dynamics: Insights from physical modeling, *J. Geophys. Res.*, *98*(B9), 16,167–16,185.

Somoza, R., and C. B. Zaffarana (2008), Mid-Cretaceous polar standstill of South America, motion of the Atlantic hotspots and the birth of the Andean cordillera, *Earth Planet. Sci. Lett.*, *271*, 267–277, doi:10.1016/j.epsl.2008.04.004.

Spalletti, L. A., and L. H. Dalla Salda (1996), A pull apart volcanic related tertiary basin, an example from the Patagonian Andes, *J. S. Am. Earth Sci.*, *9*(3–4), 197–206, doi:10.1016/0895-9811(96)00006-5.

Steinberger, B., and T. H. Torsvik (2008), Absolute plate motions and true polar wander in the absence of hotspot tracks, *Nature*, *452*(7187), 620–623, doi:10.1038/nature06824.

Stern, C. R., and M. J. de Wit (2003), Rocas Verdes ophiolites, southernmost South America: Remnants of progressive stages of development of oceanic-type crust in a continental margin back-arc basin, *Geol. Soc. Spec. Publ.*, *218*, 665–683, doi:10.1144/GSL.SP.2003.218.01.32.

Stern, C. R., and J. B. Stroup (1982), Petrochemistry of the Patagonian Batholith, Ultima Esperanza, Chile, in *Antarctic Geoscience*, edited by C. Craddock, pp. 135–147, Univ. of Wis. Press, Madison.

Suárez, M., R. de la Cruz, and C. M. Bell (2000), Timing and origin of deformation along the Patagonian fold and thrust belt, *Geol. Mag.*, *137*(04), 345–353, doi:10.1017/S0016756800004192.

Taylor, B. (2006), The single largest oceanic plateau: Ontong Java-Manihiki-Hikurangi, *Earth Planet. Sci. Lett.*, *241*(3-4), 372–380, doi:10.1016/j.epsl.2005.11.049.

Turienzo, M. M. (2010), Structural style of the Malargüe fold-and-thrust belt at the Diamante River area (34°30'–34°50'S) and its linkage with the Cordillera Frontal, Andes of central Argentina, *J. S. Am. Earth Sci.*, *29*(3), 537–556, doi:10.1016/j.jsames.2009.12.002.

Vergani, G. D., A. J. Tankard, H. J. Belotti, and H. J. Welsink (1995), Tectonic evolution and paleogeography of the Neuquén Basin, Argentina, in *Petroleum Basins of South America*, edited by A. J. Tankard, R. Suarez, and H. J. Welsink, *AAPG Mem.*, *65*, 383–402.

Vietor, T., and H. Echtler (2006), Episodic Neogene southward growth of the Andean subduction orogen between 30°S and 40°S—Plate motions, mantle flow, climate, and upper-plate structure, in *The Andes*, edited by O. Oncken, et al., pp. 375–400, Springer, Berlin, doi:10.1007/978-3-540-48684-8_18.

Villagómez, D., R. Spikings, T. Magna, A. Kammer, W. Winkler, and A. Beltrán (2011), Geochronology, geochemistry and tectonic evolution of the Western and Central Cordilleras of Colombia, *Lithos*, *125*(3–4), 875–896, doi:10.1016/j.lithos.2011.05.003.

Wessel, P., and L. W. Kroenke (2008), Pacific absolute plate motion since 145 Ma: An assessment of the fixed hot spot hypothesis, *J. Geophys. Res.*, *113*, B06101, doi:10.1029/2007jb005499.

Whitman, D., B. L. Isacks, and S. M. Kay (1996), Lithospheric structure and along-strike segmentation of the Central Andean Plateau: Seismic Q, magmatism, flexure, topography and tectonics, *Tectonophysics*, *259*(1-3), 29–40, doi:10.1016/0040-1951(95)00130-1.

Yáñez, G., and Cembrano, J., (2004), Role of viscous plate coupling in the late Tertiary Andean tectonics, *J. Geophys. Res.*, *109*, B02407, doi:10.1029/2003JB002494.

Zamora Valcarce, G., T. Zapata, D. del Pino, and A. Ansa (2006), Structural evolution and magmatic characteristics of the Agrio fold-and-thrust belt, *Geol. Soc. Am. Spec. Pap.*, *407*, 125–145, doi:10.1130/2006.2407(06).

Zapata, T., and A. Folguera (2005), Tectonic evolution of the Andean Fold and Thrust Belt of the southern Neuquén Basin, Argentina, *Geol. Soc. Spec. Publ.*, *252*(1), 37–56, doi:10.1144/gsl.sp.2005.252.01.03.